10D.5 BIMODAL PEAK IN MID-LEVEL TROPICAL LAYER CLOUDS OBSERVED BY CLOUDSAT

Emily M. Riley* and Brian E. Mapes
University of Miami, Miami, Florida

1. INTRODUCTION

The vertical distribution of clouds affects the atmosphere's radiative and latent heating profiles, which subsequently affect the large-scale circulation. Cloud structure is also a challenge and set of clues for scientific understanding, and a diagnostic target for models. Previous work has relied on infrared and visible satellite (e.g. Sheu et al. 1997), deductions from sounding data (e.g. Zuidema 1998), observations from surface and aircraft, and a few ground based radar sites to gain insights on cloud structure. With the launch of CloudSat in April 2006, direct measurements of cloud structure are now possible on the global scale (Stephens et al. 2002).

This study uses one full year (July 2006 – June 2007) of CloudSat data to examine the tropical (20°S-20°N) vertical distribution of mid-level clouds. Mid-level clouds are highlighted due to the infrequency of their observations in the past and paucity of occurrence in the literature. High and low clouds, well observed from space and from the ground, often mask the presence of mid-level clouds. CloudSat's space-based radar, discussed below, provides a unique opportunity to view clouds at all levels in the atmosphere. ECMWF sounding data along the CloudSat track and the Tropical Rainfall Measuring Mission (TRMM) product 3B42 will be used to elucidate the environmental conditions in which the mid-level clouds occur.

2. DATA AND METHODS

On board Cloudsat is a 94 GHz nadir pointing cloud-profiling radar (CPR) (Im et al. 2005) designed explicitly to detect hydrometers in the vertical. The CPR has a 1.4 km across track by 2.5 km along track nominal footprint. Vertical resolution is 480 m with backscatter oversampled to provide a resolution of 240 m. The minimal detectable signal (MDS) designed to be -28 dBZ, was found to be   -30 dBZ to -31 dBZ in early CloudSat results from Haynes and Stephens (2007). CloudSat makes approximately 14 orbits per day with an equator passing time of 0130 local local time (LT) and 1330 LT.

This study uses the 2B-GEOPROF, version 4 CloudSat product. Briefly, the 2B-GEOPROF product determines the radar reflectivity factor for significant radar echoes sampled by the CPR. Details on which echoes are deemed significant, along with a description of all CloudSat products can be found online at the CloudSat data processing center (http://cloudsat.cira.coloradostate.edu).

We view cloudiness[1] in two ways; (1) as echo objects and (2) as individual echo pixels to understand cloud distribution. An echo object is defined as a contiguous region of radar reflectivity that has at least three pixels with their edges, not corners, touching. Single and double echo pixels were initially retained in our first processing, and constituted around 63% of the pixels, but < 5% of echo area and < 1% of the echo volume. They were concentrated at low levels near topography, suggesting clutter contamination. Eliminating them seemed no great loss, while halving dataset memory requirements. For each echo object a plethora of attributes are recorded, including latitude and longitude, top and bottom height, width, and the total number of pixels contained within the object, along with the number of cells and pixels exceeding 0 dBZ and -17 dBZ (crude rain and drizzle thresholds). Geometrical and mean thickness are defined respectively as

$$\tau = (t - b) + \tau_p \quad (1)$$

$$\bar{\tau} = \left(\frac{np}{w}\right) * \tau_p \quad (2)$$

where τ, $\bar{\tau}$, are geometrical thickness, mean thickness, and t, b, np, w are top height, bottom height, number of pixels, and width. Additionally, τ_p is pixel thickness, 240 m.

ECMWF data including temperature, pressure, and specific humidity are available concurrent with CloudSat data,on a pixel-by-pixel basis. Soundings for echo objects were computed by averaging the ECMWF data over each height level in the echo

Corresponding author address: Emily M. Riley, University of Miami, Miami, FL, 33149, email: eriley@rsmas.maimi.edu

[1]We define cloudiness as the existence of significant reflectivity echo observed by the CloudSat CPR.

object. Soundings were only made for echo objects greater than 10 pixels wide to accelerate processing. Currently, we have only processed the ECMWF data from July 2006 to March 2007.

The TRMM 3B42 product provides 3-hour, 0.25°x0.25° rainfall rates, which we have re-binned to 1°x1°. The mean latitude and longitude, as well as time of each echo object observed by CloudSat are matched with the closest TRMM 3B42 rainfall rate data, allowing composites of the surrounding weather conditions to be constructed.

3. RESULTS

Figure 1 shows a histogram of echo object top height versus mean thickness for the tropics (20°S – 20°N). Both height and thickness bins are 240 m. The histogram is weighted by echo object horizontal coverage, to form a cloud-cover density. Number density is dominated by the numerous small echo objects, while the biggest echo objects dominate volume density. Cloud types are defined by slicing figure 1 into sections. We may roughly associate each section to a familiar cloud type name as follows: (a) cirrus, (b) cumulonimbus, (c) altostratus and altocumulus, (d) cumulus congestus, and (e) thin stratus clouds. Section (f) is broken into two types; wide clouds (width > 10 pixels) are stratocumulus, while narrow clouds (width < 10 pixels) are cumulus.
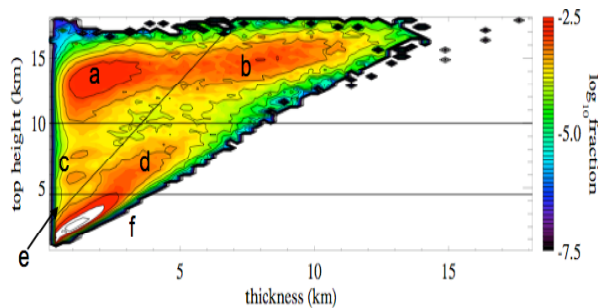

Figure 1 – Log$_{10}$ of the normalized density of cloud cover in the space of echo object top height versus echo object mean thickness, for all objects in 20°S-20°N. Horizontal lines are at 4.5 km and 10 km. The sloping line was arbitrarily specified.

The low-level echo objects have the highest fractional contribution to the distribution, due to their ubiquitous presence in the tropics. A noticeable "hole" exists in the distribution centered around 10 km height and 3 km thickness separating the low and mid-level top echo objects from the upper-level echo objects. This study focuses on the subtler feature occurring in section (c), the echo objects linked to the alto clouds. Section (c) is defined here by top height between

4.5 km and 10 km, with a thickness less than the sloping line.

A bimodal distribution for the alto cloud group is evident, with a peak in distribution between 5-6 km and another between 7-8 km, indicating there are two distinct populations of alto clouds. The bimodal distribution is a robust feature occurring when each tropical basin (i.e. Atlantic Ocean, Indian Ocean, and West and East Pacific Ocean) is viewed separately, when day and night time overpasses are viewed separately, as well as when land and ocean are viewed separtely. The alto clouds are thus subdivided into two groups; a lower population with echo object top heights between 5-6.5 km and an upper population with echo object top heights between 6.5-8 km. Echo objects in both groups must have a mean thickness less than 2 km. We have also excluded echo objects over any topography greater than 1 km, to avoid any concerns about ground altitude.

Echo objects in both the upper and lower subpopulations can be thought of as "layer" clouds, because the echo objects are thin (mean thickness < 2 km), and usually are composed of weak reflectivity (not shown; typically dBZ < 0). About 72% of these echo objects are overlapped by unconnected echoes above or below.

The geographical distribution of each sub-population is plotted in figure 2. Both occur in the deep tropical region (10°S-10°N) of the Indian and west Pacific ocean. The upper population has a max in distribution over North Africa (fig. 2a), while a broad maximum exists in the lower population between the equator and 10°N (fig. 2b). These geographical distributions somewhat resemble a map of tropical rainfall, i.e. the clouds are found around the tropical convergence zones and over the tropical warm pools. The *difference* in the location of the 6.5-8 km population and the 5-6.5 km population (Fig. 2c) indicates that the 5-6.5 km sub-population is somewhat more common in the deep tropics. Only over north Africa is the 6.5-8 km sub-population more common (c.f. 2ab). North Africa is a special case, beyond the scope of this abstract.

b)

Lower population distribution
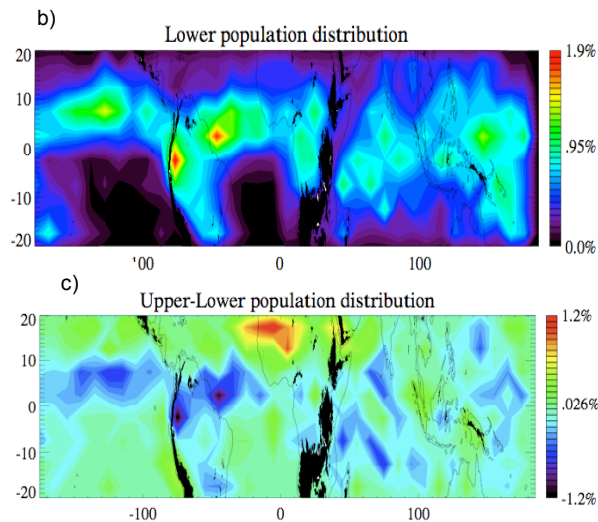
c)

Upper-Lower population distribution
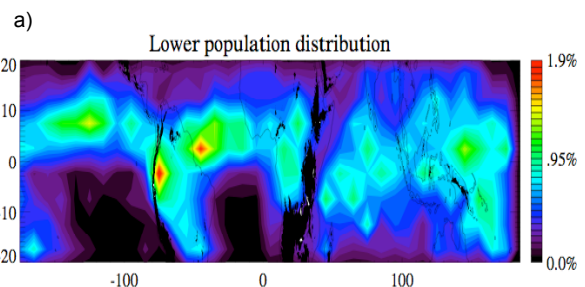
Figure 2 – Histogram of the mean latitude vs. mean longitude of (a) the 5 - 6.5 km population and (b) 6.5 - 8 km population and (c) 6.5-8 km minus the 5-6.5 km population. Units are fraction. Bin size is 5° lat X 10° lon. Echo objects over topography > 1 km have been excluded, blacked out in figure.

ECMWF data appears to reflect the presence of the two echo object populations. Figure 3a shows relative humidity profiles for echo objects in the two sub-populations. A broad increase in relative humidity occurs at approximately the observed cloud altitudes, centered slightly below the echo top heights that define the sub-populations. Spurious wiggles above 8 km are caused by pressure to height interpolation by the CloudSat processing team.

Lapse rate profiles indicate that varying stability may dictate where these mid-level layer clouds form, perhaps driven by detrainment of buoyant convection. Figure 3b shows lapse rate with height for the two sub-polulations and the tropical wide average. Three well-known stability levels are present: near the trade inversion (2 km), melting level (5 km), and tropopause (15 km) (Johnson et al. 1999). The melting level inversion is stronger near clouds with 5-6.5 tops, and may be a reason for their existence. Consistently, stability around 7 km is enhanced when clouds are observed near that level. Again we note the spurious wiggles in portions of the profile, but the signals in stability (annotated for clarity) seem clear despite that issue.
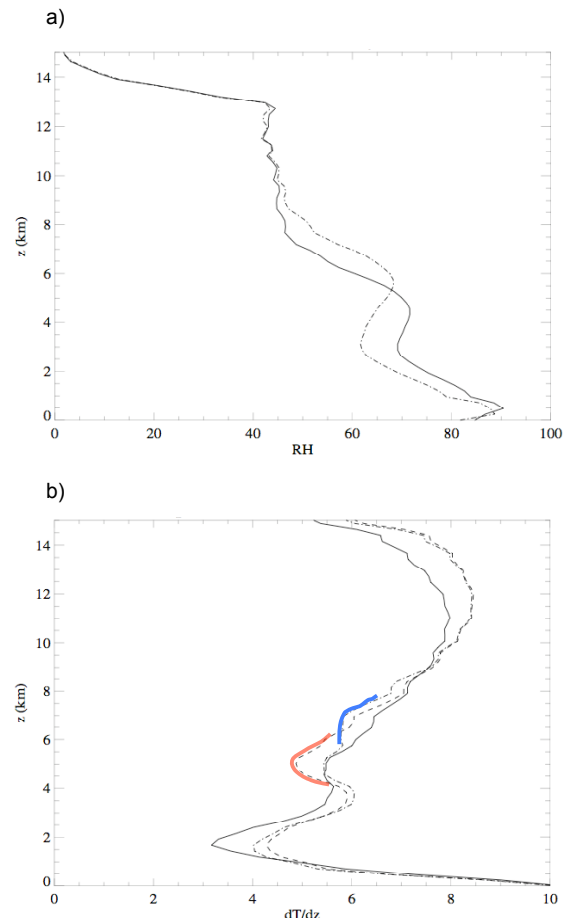
a)

b)

Figure 3 –(a) Relative humidity vs height for the lower (solid) and upper (dash-dot) population. (b) Lapse rate with height. Solid is tropical wide average, dash-dot is the 6.5-8 km cloud group, dash is 5-6.5 km cloud group. Only cases over ocean were included.

Jakob et al. (2005) showed a relationship between increasing convective activity and the presence of mid-level clouds at the Manus ARM site. Here, composites of TRMM 3B42 rain rate around echo objects in the two sub-populations indicate that both occur in association with deep convection. Both sub-populations occur approximately 1-2 days after and to the west of peak rainfall, mainly in rainfall gaps that align to form a "hole" at the origin in the rainfall composite (fig. 4). The 5-6.5 km sub-population occurs in connection with more rainy conditions (fig 4b), consistent with its deep tropics enhancement (Fig. 2c). Horizontal striations in both figures appear to reflect the diurnal variation of rainfall. Also consistently, the 5-6.5 km population has more overlapping echo pixels both above and below (not shown), indicating that it occurs in cloudier conditions on average.
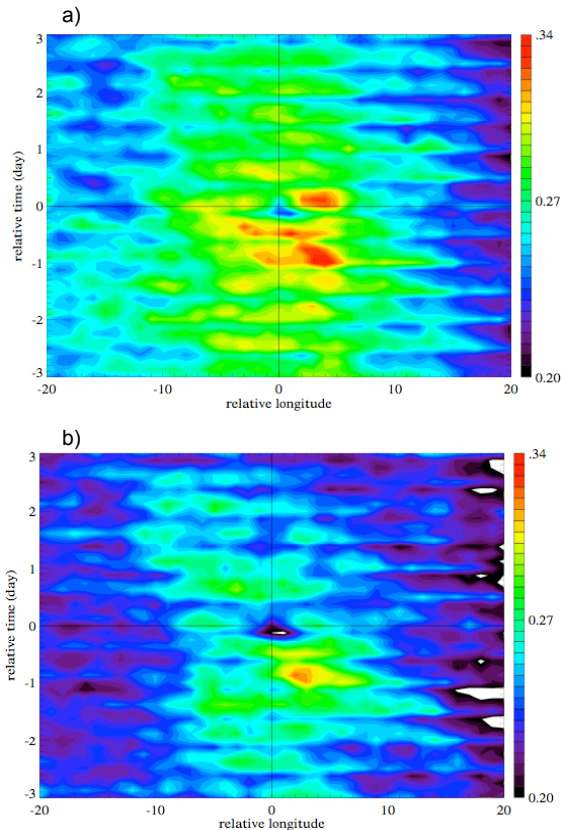
Figure 4 – TRMMS 3B42 rainfall composites for (a) 5-6.5 km population and (b) 6.5-8 km population of alto clouds. Units are mm/hr.

4. SUMMARY AND FUTURE WORK

From the above results, we conclude that there are two distinct populations in mid-level clouds throughout the tropics. Although mid-level clouds can be glimpsed in published climatologies, such as Hollars et al (2004) from the Manus ARM site, they were not mentioned and had not been identified with such statistical clarity.

These sub-populations occur in the same broad geographical patterns (fig. 2), and even in similar synoptic situations (fig. 4), but they do not actually co-occur locally, as confirmed by perusal of many cloud scenes as well as statistical overlap studies not shown here. In other words, mid-level clouds in association with convective events somehow "choose" one level or the other. The heavier rainfall around the lower sub-population may indicate that a well-developed melting inversion favors preferential detrainment and layer cloud formation at that level. This leaves the question of why, in less rainy situations, cloud top altitudes of 7-8 km are favored. The presence of stable layers in soundings is an important

observation, but raises chicken-and-egg questions that do not constitute a final explanation. Microphysical processes such as ice nucleation vs. supercooled water could also have an important hand in these preferred cloud layers.

These distinct alto clouds may be present in global weather model data, since a humidity signature is. Evidence for two layers should be sought in cloud models with sufficient resolution. If simulated, the upper layer could then be explained; if it is not simulated then more observations may be needed to advance understanding of the phenomenon. Since it is discernable at ARM sites, a wealth of other data could be brought to bear, now that the statistical significance of the two distinct sub-populations is sufficiently well established to justify the effort.

Future work will utilize a Raymond and Blyth (1992) type stochastic mixing and buoyancy sorting model to see if detrainment levels, computed for convective processes operating within the ECMWF soundings, correspond to the observations.

5. ACKNOWLEDGEMENTS

6. REFERENCES

Hollars, S., Q. Fu, J. Comsotck, and T. Ackerman, 2003: Comparison of cloud-top height retrieval from ground-based 35 GHz MMCR and GMS-5 satellite observations at ARM TWP Manus site, *Atmos. Res.*, **72**, 169-186.

Im, E., S. L. Durden, and C. Wu, 2005: Cloud profiling radar for the CloudSat mission, *IEEE Aerosp. Electron. Syst. Mag.,* **20**, 15-18.

Jakob, C., G. Tselioudis, and T. Hume, 2005: The radiative, cloud and thermodynamic properties of the major Tropical Western Pacific cloud regiems. *J. Climate*, **18**, 1203-1215.

Johnson, R. H., T. M. Rickenback, S. A. Rutledge, P. E. Ciesielski, and W. H. Schubert, 1999: Trimodal characteristics of tropical convection, *J. Climate*, **12**, 2397-2418.

Raymond, D. J., and A. M. Blyth, 1992: Extension of the stochastic mixing model to cumulonimbus clouds. *J. Atmos. Sci.*, **49**, 1968-1983.

Sheu, R. -S., J. A. Curry, and G. Liu, 1997: Vertical stratification of tropical cloud properties as determined from satellite. *J. Geophys. Res.*, **102**, 4231-4245.

Stephens, G. L., et al. 2002: The CloudSat mission and the A-train, *Bull. Am. Meteorol. Soc.*, **83**, 1771-1790.

Zuidema, P., 1998: the 600-800 minimum in tropical cloudiness observed during TOGA COARE, *J. Atmos. Sci.*, **55**, 2220-2228.